



1 Discrepancies between MICS-Asia III Simulation and Observation for
2 Surface Ozone in the Marine Atmosphere over the Northwestern Pacific
3 Asian Rim Region
4

5 Hajime Akimoto¹, Tatsuya Nagashima¹, Li Jie², Joshua S. Fu^{3,4}, and Zifa Wang²
6

- 7 1. National Institute for Environmental Studies, Onogawa, Tsukuba 305-8506, Japan
8 2. Institute of Atmospheric Physics, Chinese Academy of Sciences, Beijing 100029, China
9 3. Department of Civil and Environmental Engineering, University of Tennessee, Knoxville,
10 TN 37996, U.S.A.
11 4. Climate Change Science Institute and Computational Sciences and Engineering Division,
12 Oak Ridge national Laboratory, Oak Ridge, TN 37831, U.S.A.

13 Correspondence: Hajime Akimoto (akimoto.hajime@nies.go.jp)
14
15

16 **Abstract.** In order to identify the causes of overestimate of the surface-level O₃ mixing ratio
17 simulated by three regional chemical-transport models, namely NAQPMS v.3 (abbreviated as
18 NAQM in this paper), CMAQ v.5.0.2, and CMAQ v.4.7.1, compared to the EANET
19 observational data at a marine remote site at Oki in July 2010 in the context of MICS-Asia III,
20 analyses of hourly data of O₃ mixing ratios and net ozone production were made. In addition to
21 Oki, model-simulated and observational data for two other EANET marine sites, Hedo and
22 Ogasawara, were also examined. Three factors, i.e., long-range transport from the continent,
23 in-situ photochemical formation, and dry deposition of O₃ on seawater have been found to
24 contribute to the overestimate by these regional models at Oki. The calculated O₃ mixing ratios
25 during long-range transport from the continent were much higher for all the three models than
26 those of the observation. In-situ photochemical formation, demonstrated by a distinct diurnal
27 variation which was not discerned in the observational data, was seen in the simulated data of
28 all the three models and ascribed to the virtual transport of NO_x from the southern urban areas
29 of the main island of Japan. At Hedo and Ogasawara overestimate of O₃ in oceanic air mass was
30 found for CMAQ v.5.0.2 and v. 4.7.1, while good agreement was obtained by NAQM. The
31 overestimate by CMAQ models were inferred to be due to the use of too small dry deposition
32 rate of O₃ compared to NAQM in the Northwestern Pacific. However, the dry deposition
33 velocity of O₃ in the Bohai Bay and the Yellow Sea has been assumed to be comparable to that
34 of the open ocean in all the three models, which could have resulted in the overestimate of O₃
35 mixing ratios in this area and also in the long-range transport of O₃ from the continent to Oki. A
36 higher value of dry deposition velocity in this marine area is expected considering the higher



37 content of organics in the surface sea layer brought by rivers and atmospheric wet deposition.
38 Empirical measurements of the dry deposition flux in this area is highly recommended, since it
39 would affect the simulated mixing ratios in the down-wind region and the estimate of
40 transboundary transport of ozone from the continent to the Pacific rim region.

41

42

43

44

45

46

47

48

49

50

51

52

53

54

55

56

57



58 1 Introduction

59

60 Surface ozone simulation by regional chemical transport models (CTMs) has become
61 widely used and is thought to be well-developed considering its long history since the
62 1980s (e.g. De Wispelaer, 1981) and a well-established underlying fundamental science
63 of tropospheric gas-phase photochemistry (e.g. Akimoto, 2016). Nevertheless, a recent
64 model intercomparison study, MICS-Asia III, has revealed a large variability in the
65 simulated spatial distribution of surface O₃ mixing ratios in the East Asian region
66 among models and between models and observations (Li, J. et al., 2019). Since regional
67 CTMs are commonly used for proposing mitigation policies on how to reduce the emissions of
68 NO_x and NMVOC for controlling photochemical ozone pollution, we need to solve such
69 discrepancies among models and between models and observations.

70 We realize that model intercomparison studies of ozone simulation for air quality is
71 at the stage of identifying the causes of discrepancies and depicting the problem that are
72 used to improve models, rather than simply demonstrating the statistical performance of
73 the models and showing the degree of agreement between the simulated ensemble mean
74 and observations. Our previous paper in this special issue (Akimoto et al. 2019), noted a
75 disagreement between the observed mixing ratios of surface O₃ in the megacities of
76 Beijing and Tokyo and at a remote oceanic site at Oki, and those simulated by three selected
77 regional models, namely WRF-CMAQ, v.5.02 and v.4.7.1, and WRF-NAQPMS v.3. As for the
78 urban areas of megacities, we found that the degree of agreement of the simulated levels of O₃
79 and NO with the observations were strongly coupled, and we discussed the importance of
80 making comparisons of simulated mixing ratios of precursors (NO_x and NMVOC) together with
81 O₃ itself. Specifically, we proposed to confirm the potential importance of the heterogeneous
82 “renoxification” reaction of HNO₃ to regenerate NO_x on the aerosol surface by comprehensive
83 field observations of NO_z. We also identified that the difference in the vertical transport scheme
84 affected the simulated results of O₃ significantly.

85 As for the marine remote site of Oki, an island in the western part of Japan in the Japan Sea,
86 an overestimate of O₃ by ca. 20 ppb compared to observations in July 2010 has been noted for
87 all the three selected models. However, the causes of the disagreement between the models and
88 observations were not discussed in that paper (Akimoto et al. 2019). Oki is one of the
89 reference sites for O₃ observations, and the O₃ level there affects the estimate of the amount
90 of transboundary long-range transport of O₃ from the Asian continent to the Northwestern
91 Pacific rim region. It is also a baseline site for observations of air quality in Japan and Korea.
92 Therefore, a better matching between observational data and model simulation is preferred, and
93 elucidation of the causes of overestimates by the models is worth pursuing.



94 So far, validations of surface O₃ in the oceanic area by regional CTMs have rarely been
95 made. This is because regional CTMs have been applied mainly to the air quality in urban
96 polluted areas with the aim of controlling precursor emissions. However, in the East Asian
97 Pacific rim region, the continental outflow over the ocean is transported to the downwind area,
98 thus, a discussion of transboundary pollution is necessarily needed to validate over the oceanic
99 area. An intensive evaluation of ozone deposition simulations using regional models in East
100 Asia has been reported by Park et al. (2014), but the detailed analysis has been made mostly on
101 land area and the discussion in marine region is limited.

102 Meanwhile, since the oceans cover 2/3 of the earth surface, the air-sea exchange plays an
103 important role in the tropospheric ozone budget. The dry deposition of oceanic ozone has been
104 studied substantially by global models (Helmig et al., 2012; Sarwar et al., 2015; Luhar et al.,
105 2017; and references therein).

106 In the present study, we made a more detailed comparison of the simulated and
107 observational O₃ data in July 2010 in the marine atmosphere over the Northwestern Pacific
108 Asian Rim region. In addition to Oki, comparisons at two other oceanic sites, Hedo and
109 Ogasawara which are even more remote than Oki, have been performed. Among the selected
110 three observational sites, Ogasawara was categorized as “true oceanic site” in the North Pacific
111 Asian Rim Region (Schultz et al., 2017), Oki is a marine site affected more often by the
112 continental outflow even in the summer, and Hedo is characterised between the two sites.

113

114 2 Models and Observational Sites

115

116 The selected three models are the same as those in our previous paper, i.e., WRF-CMAQ v.5.0.2,
117 v.4.7.1, and WRF-NAQPMS v.3 (abbreviated as NAQM hereafter in this paper). Model
118 calculations by the CMAQ v.5.0.2, v.4.7.1, and NAQM were conducted at the University of
119 Tennessee (USA), National Institute for Environmental Studies (Japan), and Institute of
120 Atmospheric Physics (China), respectively. Basic features and the simulated domain of these
121 regional models have been given in previous papers in this special issue (Akimoto et al., 2019;
122 Li, J. et al., 2019). Briefly, the employed horizontal resolution was 45 km for all the models.
123 The models employed the common meteorological fields from WRF simulations and common
124 emissions of MIX (0.25° × 0.25°) for 2010 (Li, M. et al., 2017) both developed in the
125 MICS-Asia III project. The initial and boundary conditions were supplied by global models,
126 CHASER for CMAQ v.4.7.1 and NAQM, and GEOS-Chem for CMAQ v.5.0.2.

127 Three observational sites of EANET (Acid Deposition Monitoring Network in East Asia) at
128 Oki (36.3°N, 133.2°E, 90m asl), Hedo (26.9°N, 128.2°E, 60m asl), and Ogasawara (27.1°N,
129 142.2°E, 212m asl) ([www.eanet.asia/about/site information/](http://www.eanet.asia/about/site-information/)) (See Fig. 1) were selected for the

Fig. 1



130 comparison of observational data with model simulation. The Oki station is on the northern cliff
131 of Dogo Island of Oki Islands, the Hedo station is at Cape Hedo located at the northern tip of
132 Okinawa main island, and the Ogasawara station is on the hill of Chichi Island of Ogasawara
133 Islands. Measurements of O₃ were made by using UV absorption instruments (Horiba
134 APOA-360, -370). The observational data used for the three sites were the 1-hr averaged values
135 in July 2010, provided by the EANET Network Center, Asia Center for Air Pollution Research
136 (ACAP) (<http://www.acap.asia>).

137

138 **3 Results and Discussion**

139

140 **3.1 Comparison of O₃ at Oki, Hedo, and Ogasawara**

141

142 Figures 2 a-c depict the comparison of the monthly mean diurnal variation of surface O₃ mixing
143 ratios in July 2010 between the model simulations and observations at Oki, Hedo, and
144 Ogasawara, respectively. The data shown in Fig. 2a at Oki is the same as that presented in our
145 previous paper (Akimoto et al., 2019), and indicates that the O₃ mixing ratios simulated by all
146 three models fall within the range of ~10 ppbv at the 52–71 ppbv level, as compared to the
147 observational value of 34–43 ppbv. Thus, all three models overestimated the O₃ mixing ratio by
148 nearly 20–30 ppbv. A monthly averaged diurnal amplitude of 17 and 15 ppbv with a daytime
149 maximum and a nighttime minimum can be noted for CMAQ 5.0.2 and NAQM, which is
150 substantially larger than the variability of 7 and 9 ppbv for the simulation by CMAQ 4.7.1 and
151 the observation, respectively.

152 In contrast to Oki, the monthly-averaged observational mixing ratios of O₃ at Hedo and
153 Ogasawara are approximately in the same range, 12–16, and 10–14 ppbv, respectively, with a
154 slight diurnal variation of ca.4 ppbv. The model simulation of NAQM reproduced well the
155 monthly-averaged O₃ levels at these sites with almost no diurnal variation (ca. 4 and 1 ppbv at
156 Hedo and Ogasawara, respectively). Meanwhile, CMAQ 5.0.2 and 4.7.1 agree well with each
157 other, but overestimate the observed monthly-averaged O₃ mixing ratios by nearly 23–27 ppb at
158 Hedo and 11–14 ppbv at Ogasawara. These models show a diurnal variation of 9–16 ppbv at
159 Hedo, overestimating the observation substantially. The diurnal variation revealed by these
160 models at Ogasawara is less than 1 ppb, agreeing well with NAQM.

161 In order to clarify the causes of the discrepancies, comparisons of the mixing ratios of O₃ on
162 an hourly basis were made at Oki, Hedo, and Ogasawara (Figs. 3 a-c). In the observational data
163 at Oki shown in Fig. 3a, minimum mixing ratios of ca. 20 ppb are often seen within a short time
164 duration of a few hours, which represents the O₃ level in the marine air mass brought by the
165 southerly wind of the summer monsoon from the surrounding oceanic area near Japan, as

Fig. 2

Fig. 3



166 revealed by Akimoto et al. (1996). The observational data also shows that the O₃ mixing ratio at
167 Oki often reaches the level of ca. 60 ppbv, and the highest O₃ level of ca. 80ppbv was observed
168 on July 6-8. This event is thought to be caused by the long-range transport from the continent
169 (cf. Akimoto et al., 1996). The model simulations captured this event, but the estimated peak
170 height of O₃ on July 6-7 is much higher, more than 130 ppbv by CMAQ 5.0.2, and ca 100 ppbv
171 by NAQM and CMAQ 4.7.1.

172 As seen in Fig. 3(a), a distinct diurnal variation with a daytime maximum and a nighttime
173 minimum can be discerned during July16-20 in the simulations by NAQM and CMAQ 5.0.2.
174 The diurnal variation is less profound in the CMAQ 4.7.1 simulation and is not discernible in
175 the observational data. This feature apparent in the model simulations is thought to be the result
176 of in-situ photochemical O₃ production during daytime, caused by overestimated NO_x mixing
177 ratios by the models, as will be discussed later in 3.3.

178 At Hedo on Okinawa island, the observation shows that the minimum (baseline) mixing ratio
179 of O₃ in the maritime air mass in this region is 5-10 ppb in July (Fig. 3b). The figure also shows
180 that the observational O₃ level frequently reaches 20-30 ppbv. NAQM reproduced well the
181 background marine O₃ levels of ca. 10 ppbv and the higher O₃ levels of 20-30 ppbv. In contrast,
182 a strong diurnal variation is apparent in the CMAQ 5.0.2 simulation with an amplitude of more
183 than 20 ppbv, and also in the CMAQ 4.7.1 simulation with a slightly less amplitude.
184 Furthermore, the maritime background O₃ level simulated by these models is ca. 20 ppbv, nearly
185 10 ppb higher than the observation. These values of the diurnal variation and background level
186 clearly indicate an overestimate of monthly mean O₃ levels by more than 20 ppbv (Fig. 2b).

187 At Ogasawara, a more remote site in the Northwestern Pacific about 1000 km south of
188 Tokyo, the observational O₃ mixing ratios in the oceanic air are 2-8 ppbv (Fig. 3c). However,
189 even at Ogasawara in summer, higher O₃ mixing ratios up to 30 ppbv have been observed. The
190 less than 10 ppbv baseline level of O₃ in the remote oceanic air in this region is well reproduced
191 by NAQM, but CMAQ 5.0.2 and 4.7.2 give more than 10 ppbv higher values than the
192 observation. All three models captured well the observed O₃ peak on July 23-24, which can be
193 ascribed to long-range transport from Japan, as will be discussed in 3.2 below. NAQM
194 reproduced well the observed maximum O₃ mixing ratio of ca. 30 ppb as well as the transport
195 amplitude of ~25 ppbv. CMAQs gave the similar transport amplitude of ~25 ppbv, but the
196 overestimated the peak values due to the overestimate of the baseline mixing ratios. As a result,
197 the NAQM-simulated values of monthly mean mixing ratios match excellently the observations,
198 however the CMAQ 5.0.2 and 4.7.1 simulations give ca. 15 ppbv higher O₃ values at
199 Ogasawara in July (Fig. 2c).

200 From these results, we consider that three factors, long-range transport, in-situ
201 photochemical O₃ formation, and background mixing ratio of oceanic O₃ which is affected by



202 dry deposition of O₃ on seawater, would be related to the overestimate of surface O₃ at Oki in
203 July by the selected three models in the MICS-Asia III.

204

205 **3.2 Long-range transport of O₃**

206

207 At least two high O₃ events, one at Oki between July 6 and 8 and the other at Ogasawara on July
208 23 and 24 are thought to be caused by long-range transport of O₃. In order to confirm the
209 characteristics of these events, the spatial distribution of surface O₃ in East Asia obtained by
210 CMAQ 4.7.1 at 18 JST on July 6 and at 19 JST on July 23, are shown in Figs. 4a and b,
211 respectively. Fig. 4a shows that the plume of continental outflow is transported to the Yellow
212 Sea, South Korea and Japan covering the Oki site. In this event, the simulated surface O₃ mixing
213 ratios by NAQM, CMAQ 5.0.2 and 4.7.1 are 104, 135 and 110 ppbv, respectively, which are
214 substantially higher than the observational value of 80 ppbv. An overestimate of the O₃
215 level in the upwind area of Beijing produced by CMAQ 5.0.2 and 4.7.1 has been identified in
216 our previous paper (Akimoto et al., 2019), which may have contributed to some extent to the
217 overestimate of O₃ by these models during this event. On the other hand, NAQM reproduced
218 well the O₃ levels in the urban areas of Beijing in July (Akimoto et al., 2019). Nevertheless, the
219 simulated level of O₃ by NAQM during the event is ca. 20 ppbv higher than that of the
220 observation, which implies that an additional factor contributes to the overestimate of O₃ in the
221 long-range-transported air mass.

222 This additional factor of the overestimate of surface O₃ in the long-range-transported O₃
223 from the continent commonly affecting the results of all of the three selected models is thought
224 to be the result of the overestimate of surface O₃ over the Bohai Sea, Yellow Sea, and the
225 southern part of the Sea of Japan caused by the underestimate of dry deposition velocity of O₃
226 over the seawater, which will be discussed in detail later in 3.4.

227 Fig. 4b shows the long-range transport of O₃ over Japan to the Ogasawara islands on July 23.
228 Under certain meteorological conditions, a high level of O₃ over Japan is transported southward
229 toward the Pacific Ocean along with the edge of the Pacific High. The simulations of the
230 amounts of transported O₃ to Ogasawara by all the three models reproduce the observed value
231 of ~25 ppbv reasonably well, and the long-range transport of O₃ from Japan in this region is not
232 overestimated in either of the models.

233

234 **3.3 In-situ photochemical formation of O₃**

235

236 An apparent diurnal variation of O₃ with a daytime maximum and a nighttime minimum
237 have been noted in the simulated results at Oki in Fig. 3a for all three models particularly during

Fig. 4



238 July 16-23, which is not distinctly discerned in the observational data. Such a diurnal variation
239 in the simulated results strongly suggests that an in-situ photochemical buildup of O₃ occurs in
240 the model simulations. In order to assess the extent of the photochemical buildup and net
241 chemical production of O₃ at the remote marine site of Oki, the model-simulated mixing ratio of
242 NO_x has been compared with the observational data (Fig. 5). Figure 5a depicts the mixing ratio
243 of NO₂^{*} and NO observed using a chemiluminescent analyzer with Molybdenum (Mo)
244 catalyzer. Since the Mo catalyzer reduces not only NO₂ but also gaseous HNO₃ and particulate
245 NO₃⁻ to NO in an unstoichiometric way, the quantity of NO₂^{*} rather than NO₂ is reported in the
246 EANET protocol. Since the contribution of HNO₃ to NO₂^{*} is significant at remote sites, it is not
247 possible to assess the exact ratio of NO₂/NO₂^{*}, thus, NO₂^{*} should be used only as a rule of
248 thumb for the upper limit of NO₂. Fig. 5b, c, and d show the NO and NO₂ at Oki calculated by
249 NAQM, CMAQ 5.0.2 and 4.7.2, respectively.

Fig. 5

250 As can be seen in these figures, all the simulated data show significant levels of NO₂ over 2
251 ppbv in the period from July 16 to 21, which is substantially higher than the observed NO₂^{*}
252 which is typically lower than 2 ppbv. It should be noted that the temporal variation of NO₂ in
253 the simulations by CMAQ 5.0.2 and 4.7.1 is similar, but the absolute mixing ratio simulated by
254 CMAQ 5.0.2 is substantially higher than that simulated by CMAQ 4.7.1. Meanwhile, the
255 temporal pattern of the NO₂ mixing ratios simulated by NAQM is quite different from that
256 simulated by CMAQs, and a significantly high level of NO₂ up to 11 ppbv can be seen on July
257 13.

258 It should be pointed out that Oki station is a remote site and the emission of NO_x within the
259 model grid covering Oki is very low, which gives a low simulated mixing ratio of NO₂ of less
260 than 1 ppbv in the early half of the month, as typically seen in CMAQs simulations (Figs. 5c
261 and d). Since all three models use the same emission data supplied by the MICS-Asia III project
262 (Li, M., 2017), the high NO₂ seen in Figs. 5b-d is thought to be transported from
263 urban/industrial sources nearby. A possible source is Matsue and surrounding cities in mainland
264 Japan, less than 100 km south of the Oki site. Model simulations of meteorology may produce a
265 high NO_x value from this area, which does not happen in reality. The different temporal pattern
266 of NO_x between the NAQM and CMAQ simulations is thought to result from the difference in
267 the coupling of transport and chemistry in these models. A high NO₂/NO ratio seen in the model
268 simulation is consistent with the estimate that the virtual source area of NO_x is not close to the
269 site on the island.

270 Figures 6a-c depict the hourly net chemical production of O₃ at Oki in July calculated by
271 NAQM, CMAQ 5.0.2, and CMAQ 4.7.1, respectively. A substantial photochemical O₃
272 production was simulated by NAQM and CMAQ 5.0.2 up to more than 15 ppb hr⁻¹ and a
273 smaller amount of less than ca. 10 ppbv by CMAQ 4.7.1 corresponding to the simulated NO_x

Fig. 6



274 mixing ratios. Such in-situ net production during daytime shows a distinct diurnal variation for
275 the simulated mixing ratios of O_3 during a certain period in July. Thus, virtually simulated
276 relatively high NO_x implies in-situ photochemical O_3 production, which contributes to the
277 overestimate of the monthly-averaged mixing ratio of O_3 at Oki by all the three models.

278 An analysis reveals that the situation is similar at Hedo. Photochemical O_3 production up to
279 ~ 10 ppb hr^{-1} has been simulated by CMAQ 5.0.2 (Fig. 7a). A net photochemical O_3 production
280 has been simulated by CMAQ 4.7.1 and NAQM to a lesser extent (not shown). Although Hedo
281 is also a remote island site, the area surrounding the station consists of sugar cane fields and the
282 soils emit substantial NO_x (Matsumoto et al., 2001), resulting in some diurnal O_3 formation in
283 the observational data as shown in Fig. 3b. The substantial overestimate of the photochemical
284 O_3 formation at Hedo produced by CMAQ 5.0.2 and 4.7.1 as revealed by the distinct diurnal
285 variation of O_3 in Fig 3b, may be due to the virtual transport of NO_x from urban areas in the
286 southerly part of Okinawa island, as in the case of Oki. The overestimate of the in-situ
287 photochemical buildup of O_3 seems to have resulted from an overestimate of more than ca. 10
288 ppb in the monthly mean mixing ratios by these models in addition to the overestimate of the
289 background levels.

290 At Ogasawara, no such photochemical buildup of O_3 can be seen by any of the models, as
291 demonstrated for CMAQ 5.0.2 in Fig. 7c. The overestimate of background O_3 in clean marine
292 air mass gives a value of ca.10 ppbv monthly mean O_3 by the CMAQ models (Fig. 2c).

293

294 3.4 Dry deposition of O_3 on seawater

295

296 Figures 8a-c compare the spatial distribution of monthly mean surface ozone mixing ratios in
297 July 2010 in the coastal and oceanic areas of East Asia calculated by NAQM, CMAQ 5.0.2, and
298 4.7.1, respectively. A large variability in the O_3 mixing ratio among the models can be seen in
299 heavily polluted land areas, and possible causes of the difference in the megacities of Beijing
300 and Tokyo have been discussed in our previous paper (Akimoto et al., 2019). In addition to the
301 land area, a difference of surface O_3 mixing ratios in the oceanic area among the three models
302 can be seen in the figures. The NAQM-simulated surface O_3 in the open oceanic area south of
303 Japan is 10-15 ppbv, which is substantially lower than the 25-30 ppbv produced by CMAQ
304 5.0.2 and 4.7.1. These values correspond well to the monthly mean O_3 mixing ratios at the “true
305 oceanic site” Ogasawara, shown in Fig. 2c. Figure 8 also shows that Cape Hedo in Okinawa is
306 at the edge of the Pacific marine airmass with the lowest O_3 , where the coastal airmass is
307 affected by the continental outflow. The O_3 mixing ratio near this site simulated by CMAQ 5.0.2
308 and 4.7.1 is 30-40 ppbv as compared to ca. 10-20 ppbv calculated by NAQM, which
309 corresponds well with the monthly mean values at Hedo (Fig. 2b).

Fig. 7

Fig. 8



310 Thus, the overestimate of surface ozone at the oceanic sites of Hedo and Ogasawara
311 produced by the CMAQ models shown in Fig. 8 are ascribed to an overestimate of O₃ in the
312 vast area of the open Pacific Ocean. We speculate that this overestimate is caused by an
313 underestimate of dry deposition velocity of O₃ on seawater made by these models. Although the
314 discussion of the impact of dry deposition to oceanic water on the surface ozone mixing ratio
315 calculated by regional models is limited, the impact simulated by global models has been
316 studied rather extensively (Sarwar et al., 2015; Luhar et al., 2017, and references therein), since
317 oceans cover 2/3 of the earth surface, and thus the air-sea exchange plays an important role in
318 the tropospheric ozone budget. The latter studies revealed that large uncertainties exist in the
319 magnitude of the air-sea exchange of ozone with the deposition velocity (V_d) ranging from
320 0.01 to 0.15 cm s⁻¹ for oceanic water and 0.01–0.1 cm s⁻¹ for freshwater [Ganzeveld et al., 2009].
321 Typically applied values for V_d over the ocean in global models are in the range of ~0.013 to
322 0.05 cm s⁻¹ [Ganzeveld and Lelieveld, 1995].

323 Although direct measurements of the ozone deposition flux over the ocean are limited,
324 Helmig et al (2012) conducted a ship-based eddy covariance ozone flux measurement on five
325 cruises covering the Gulf of Mexico, the southern and northern Atlantic, the Southern Ocean
326 and the eastern Pacific along Chile. The median V_d for four cruises falls within the range of
327 0.01–0.02 cm s⁻¹ in the off-coast ocean area, while the median V_d measured in the coastal zone
328 fell within the range of 0.24 ± 0.02 cm s⁻¹ (Helmig et al., 2012). These findings clearly show a
329 tendency of increasing ozone deposition in the coastal zone, agreeing with the suggestion that
330 there is a gradient of ozone deposition velocity which decreases with increasing distance from
331 the coast (Ganzeveld et al., 2009).

332 Ganzeveld et al. (2009) suggested that dissolved iodine and unsaturated organic compounds
333 are key factors in driving the oceanic ozone uptake. The impact of enhanced ozone deposition
334 and halogen chemistry on tropospheric ozone over the Northern Hemisphere has also been
335 discussed by Sarwar et al. (2015). Coleman et al. (2010) applied a process-based mechanism
336 focusing on the role of oceanic deposition over the northeastern Atlantic Ocean using a
337 regional-scale model. Another study that focused on the effect of dry deposition of O₃ on the
338 ocean in the northwestern Gulf of Mexico using CMAQ has also been reported. A modified
339 module including iodide reaction showed a significant increase in the velocity of the dry
340 deposition of O₃ onto the sea surface (Oh et al., 2008).

341 In order to discuss the effect of dry deposition of O₃ over the seawater, the spatial
342 distribution of monthly-averaged V_d in the continental rim region of the Northwest Pacific
343 Ocean was simulated by NAQM, CMAQ 5.0.2, and 4.7.1 in Fig. 9a-c, respectively. The
344 simulated V_d of O₃ has been calculated by

Fig. 9



345
$$V_d = \frac{F_{O_3}}{[O_3]} \quad (1)$$

346 where F_{O_3} is the downward deposition flux of O_3 (ppbv s cm^{-1}) and $[O_3]$ is the monthly mean
347 surface O_3 mixing ratio (ppbv). Figure 9 shows that the V_d over the Northwestern Pacific Ocean
348 south of Japan is typically 0.0015-0.002 $cm\ s^{-1}$ in the NAQM simulation and 0.0005-0.001 cm
349 s^{-1} in the CMAQ 5.0.2, and 4.7.1 simulations. Thus, the values used by NAQM are about twice
350 as large as those used by CMAQs. Although even the values used by NAQM are nearly one
351 order of magnitude smaller than the measured values (0.01-0.02 $cm\ s^{-1}$) in the Atlantic open
352 ocean by Helmig et al. (2012), the better reproduction of observed O_3 mixing ratios at Hedo and
353 Ogasawara by NAQM simulations could be ascribed to a twice as large deposition velocity as
354 that in CMAQs.

355 It can be noted that the mixing ratios of O_3 in the Bohai Bay and the Yellow Sea shown in
356 Figs. 8a-c are relatively high for all the three models as compared to the surrounding land area.
357 This may be caused by the use of a much smaller deposition velocity of O_3 over the ocean
358 closer to the continent. While iodine has been evaluated to be most important in increasing the
359 dry deposition velocity of O_3 over the ocean, dissolved organic carbon is also thought to
360 contribute significantly to this process (Ganzeveld et al., 2009; Sarwar et al, 2016). Thus, the
361 dry deposition velocity of O_3 in the Bohai Bay and the Yellow Sea is expected to be much
362 higher than that in the open Pacific Ocean. However, as shown in Fig. 9, the dry deposition
363 velocity in this area employed by all the three models is even smaller than that in the open
364 Pacific Ocean. This is unreasonable considering the discussion by Ganzeveld et al. (2009)
365 which has been supported by the findings of Helmig et al. (2012). Particularly, the even lower
366 deposition velocity in this area assumed by NAQM compared to that in the open Pacific would
367 have contributed substantially to the overestimate of O_3 at Oki by this model.

368 The overestimate of O_3 mixing ratio in the Bohai Bay and Yellow Sea definitely contributes
369 to the overestimate of O_3 at Oki and to the evaluation of transboundary long-range transport of
370 O_3 to Korea and Japan. Since the model is highly sensitive to water surface resistance, it is
371 important to empirically obtain the values of dry deposition flux of O_3 and its precursors over
372 the Bohai Bay and the Yellow Sea.

373 In addition to the dry deposition on sea water, photochemical gas-phase halogen chemistry
374 mainly by iodine has been suggested to decrease surface O_3 in the northern hemisphere
375 substantially (Sarwar et al., 2015). Since no sensitivity analysis of the impact of dry deposition
376 velocity and gas-phase halogen photochemistry has been made in MICS-Asia III, future studies
377 will be necessary to resolve the issue.

378

379 **4 Future Research Recommendations**



380

381 The present and the previous paper (Akimoto et al., 2019) aimed to elucidate the causes of
382 discrepancies of surface-level ozone at remote marine sites and central megacity sites in East
383 Asia, respectively, among models and between models and observation. Based on the findings
384 in these analyses, a couple of future research recommendations are proposed here in order to
385 solve the issues encountered in model intercomparison studies on surface-level ozone.

386 1. Measurement of dry deposition flux of O₃ over the Bohai Bay and the Yellow Sea

387 Surface-level ozone mixing ratios in the marine region of East Asia have been found to be
388 sensitive to the dry deposition velocity of O₃ over seawater. Although the dry deposition
389 velocity over the Bohai Bay and the Yellow Sea is expected to be much larger than that over
390 the open ocean in the Northwestern Pacific due to the enriched organic compounds brought
391 by rivers and atmospheric wet deposition, no such measurements have been conducted to
392 our knowledge. Since the dry deposition velocity of O₃ over the Bohai Bay and the Yellow
393 Sea affects the evaluation of trans-boundary transport of O₃ to the down-wind region, the
394 measurement of V_d in this marine area is highly recommended.

395 2. Simultaneous comprehensive measurement of NO_y focusing on gaseous HNO₃ in urban
396 areas

397 In order to perform reliable model simulation of surface-level ozone in urban areas for the
398 purpose of proposing an ozone control policy, it is important to verify if NO_y chemistry is
399 properly incorporated. In particular, model validation for HNO₃ is important, since the
400 mixing ratio of gaseous HNO₃ is estimated to be comparable to NO_x. However, due to
401 technical difficulty, no direct measurement of gaseous HNO₃ together with other NO_y has
402 been conducted. Field campaign in urban areas for simultaneous measurement of NO_y
403 including direct measurement of gaseous HNO₃ (e.g. by chemical ionization mass
404 spectrometry) is highly recommended focusing on the quantification of the potential
405 importance of the heterogeneous “renoxification” reaction of HNO₃ to regenerate NO_x on
406 the aerosol surface.

407 These activities are recommended to be jointly co-organized by field experimentalists and
408 modelers.

409

410 5 Summary

411

412 Simulations by the regional chemical transport models, NAQM, CMAQ v.5.0.2 and CMAQ
413 v.4.7.1, in the context of MICS Asia III overestimated the observed surface-level ozone at Oki
414 in July 2010 by 20-30 ppbv. In order to identify the causes of this overestimate, analyses were
415 performed not only for Oki but for two other EANET marine sites, Hedo and Ogasawara as well.



416 At Hedo and Ogasawara, NAQM reproduced well the observational values of monthly mean
417 diurnal mixing ratios of O₃, while the two CMAQ models overestimated the observation by
418 23-27 ppbv and 11-14 ppbv, respectively.

419 Three factors have been identified as the cause of overestimate made by the model
420 simulations at Oki; (i) long-range transport of O₃ from the continent, (ii) in-situ photochemical
421 formation of O₃, and (iii) dry deposition of O₃ on seawater. An overestimate of transported O₃
422 from the continent can be identified for all the three models. The overestimate for the CMAQ
423 models can be ascribed partly to an overestimate of the O₃ mixing ratio in the source region of
424 China, as discussed in our previous paper (Akimoto, 2019). An overestimate of
425 long-range-transported O₃ was also seen in NAQM which reproduced the mixing ratio in
426 Beijing reasonably well. The cause of overestimate of long-range-transported O₃ by NAQM was
427 ascribed to the possible overestimate of O₃ in the Bohai Bay and Yellow Sea due to the too
428 small deposition velocity of O₃ over the seawater in this region assumed in the model.

429 The overestimate of the monthly-averaged mixing ratio of O₃ at Oki has been ascribed
430 partly to the in-situ photochemical formation, which was demonstrated by the distinct diurnal
431 variation of O₃ produced by all the three models but not discernible in the observational data.
432 Such an in-situ formation of O₃ was found to be caused by the virtual transport of NO_x in the
433 model simulation from the urban areas of mainland Japan to Oki.

434 At Hedo and Ogasawara sites, an overestimate of O₃ in the oceanic air mass was found in
435 CMAQ 5.0.2 and 4.7.1, while a good agreement with observational data was obtained by
436 NAQM. The overestimate by the CMAQ models was ascribed to the employment of too small
437 dry deposition velocity of O₃ on seawater, while the use of a larger deposition velocity by
438 NAQM may have resulted in a good agreement with the observation. It has been identified that
439 O₃ mixing ratios over the Bohai Bay and the Yellow Sea are higher than those over the
440 surrounding land surface for all the three models, which was ascribed to the employment of too
441 small dry deposition velocity on seawater in this area in spite of higher contents of organics due
442 to the rivers and atmospheric deposition.

443

444 *Data availability.* The EANET observational dataset used in this study is available at
445 <http://www.eanet.asia>.

446

447 *Author contributions.* HA analyzed the data and wrote the first draft of the paper. TN, JL, and
448 JSF provided the model simulation data for their own models and conducted discussions for the
449 paper. ZW contributed to the availability of modeling data as a coordinator of MICS-Asia III.

450

451 *Competing interests.* The authors declare that they have no conflict of interest.



452

453 *Special issue statement.* This article is part of the special issue “Regional assessment of air
454 pollution and climate change over East and Southeast Asia: results from MICS-Asia Phase III”.

455 It is not associated with a conference.

456

457 *Financial support.* This research was supported by the Environment Research and Technology
458 Development Fund (S12-1) of the Ministry of the Environment, Japan, and by the Natural
459 Science Foundation of China (41620104008).

460

461 *Review statement.*

462

463

464 **References**

465

466 Akimoto, H., Atmospheric Reaction Chemistry, Springer Japan, Tokyo, 2016.

467 Akimoto, H. and Hirokawa, J., Atmospheric Multiphase Chemistry - Fundamentals of
468 Secondary Aerosol Formation -, John Wiley & Sons, 2020. (in press)

469 Akimoto, H., Mukai, H., Nishikawa, M., Murano, K., Hatakeyama, S. Liu, C.-M.,
470 Buhr, M. Hsu, K. J., Merrill, J. T., and Newell, R. J., Long-range transport of
471 ozone in the East Asian Pacific rim region, J. Geophys. Res., 101, 1999-2010,
472 1996.

473 Akimoto, H., Nagashima, T., Li, J., Fu J. S., Ji, D., Tan, J., and Wang Z., Comparison of Surface
474 Ozone Simulation among Selected Regional Models in MICS-Asia III – Effects of Chemistry
475 and Vertical Transport for the Causes of Difference-, Atmos. Chem. Phys., 19, 603–615,
476 2019.

477 Coleman, L., Varghese, S., Jennings, S. G., and O'Dowd, C. D., Regional-scale ozone deposition
478 to north-east Atlantic waters, Adv. Meteorol., 243701, 16 pp., [http://dx.doi.org/10.1155/2010/](http://dx.doi.org/10.1155/2010/243701)
479 243701, 2010.

480 De Wispelaer, C/, Ed., Air Pollution Modeling and its Application I, Plenum Press, New York,
481 1981.

482 EANET, EANET site information <https://www.eanet.asia/about/site-information/>
483 (last access: 23 January 2020).

484 Ganzeveld, L. and J. Lelieveld, Dry deposition parameterization in a chemistry general
485 circulation model and its influence on the distribution of reactive trace species, J. Geophys.
486 Res., 100, 20,999–21,012, doi:10.1029/95JD02266, 1995.

487 Ganzeveld, I., Helmig, D., Fairall, C. W., Hare, J., and Pozzer, A., Atmosphere-ocean ozone



- 488 exchange: A global modeling study of biogeochemical, atmospheric, and waterside
489 turbulence dependencies, *Global Biogeochem. Cycles*, 23, GB4021, pp.16,
490 doi:10.1029/2008GB003301, 2009.
- 491 Helmig, D., Lang, E. K., Bariteau, L., Boylan, P., Fairall, C. W., Ganzeveld, L., Hare, J. E.,
492 Hueber, J., and Pallandt, M., Atmosphere-ocean ozone fluxes during the TexAQS 2006,
493 STRATUS 2006, GOMECC 2007, GasEx 2008, and AMMA 2008 cruises, *J. Geophys. Res.*,
494 117, D04305, <https://doi.org/10.1029/2011JD015955>, 2012.
- 495 Li, J., Nagashima, T., Kong, L., Ge, B., Yamaji, K., Fu, J. S., Wang, X., Fan, Q., Itahashi, S.,
496 Lee, H.-J., Kim, C.-H. Lin, C.-Y., Zhang, M., Tao, Z., Kajino, M., Liao, H., Li, M., Woo,
497 J.-H., Kurokawa, J., Wang, Z. Wu, Q., Akimoto, H. Carmichael, G. R., and Wang, Z., Model
498 evaluation and intercomparison of surface-level ozone and relevant species in East Asia in
499 the context of MICS-Asia Phase III – Part I: Overview, *Atmos. Chem. Phys.* 19,
500 12993-13015, 2019.
- 501 Li, M., Zhang, Q., Kurokawa, J., Woo, J.-H., He, K. B., Lu, Z., Ohara, T., Song, Y., Streets, D.
502 G., Carmichael, G. R., Cheng, Y. F., Hong, C. P., Huo, H., Jiang, X. J., Kang, S. C., Liu, F.,
503 Su, H., and Zheng, B., MIX: a mosaic Asian anthropogenic emission inventory for the
504 MICS-Asia and the HTAP projects, *Atmos. Chem. Phys.* 17, 935-963, 2017.
- 505 Luhar, A. K., Galbally, I. E., Woodhouse, M. T., and Thatcher, M., An improved
506 parameterisation of ozone dry deposition to the ocean and its impact in a global climate–
507 chemistry model, *Atmos. Chem. Phys.*, 17, 3749–3767, 2017.
- 508 Matsumoto, J., Hirokawa, J., Akimoto, H., and Kajii, Y., Direct measurement of NO₂ in the
509 marine atmosphere by laser-induced fluorescence technique, *Atmos. Environ.* 35, 2803-2814,
510 2001.
- 511 Oh, I.-B., Byun, D. W., Kim, H.-C., Kim, S., and Cameron, B., Modeling the effect of iodide
512 distribution on ozone deposition to seawater surface, *Atmos. Environ.*, 42, 4453–4466, 2008.
- 513 Park, R. J., Hong, S. K., Kwon, H.-A., Kim, S., Guenther, A., Woo, J.-H., and Loughner, C. P.,
514 An evaluation of ozone dry deposition simulations in East Asia, *Atmos. Chem. Phys.*, 14,
515 7929-7940, 2014.
- 516 Pleim, J. E., Xiu, A., Finkelstein, P. L., and Otte, T. L., A coupled land-surface and dry
517 deposition model and comparison to field measurements of surface heat, moisture, and ozone
518 fluxes, *Water Air Soil Pollut.*, 1, 243–252, 2001.
- 519 Sarwar, G., Gantt, B., Schwede, D., Foley, K., Mathur, R., and Saiz-Lopez, A., Impact of
520 enhanced ozone deposition and halogen chemistry on tropospheric ozone over the Northern
521 Hemisphere, *Environ. Sci. Technol.* 49, 9203-9211, 2015.
- 522 Wesely, M. L., Parameterization of surface resistances to gaseous dry deposition in
523 regional-scale numerical models, *Atmos. Environ.*, 23, 1293-1304, 1989.



Figures

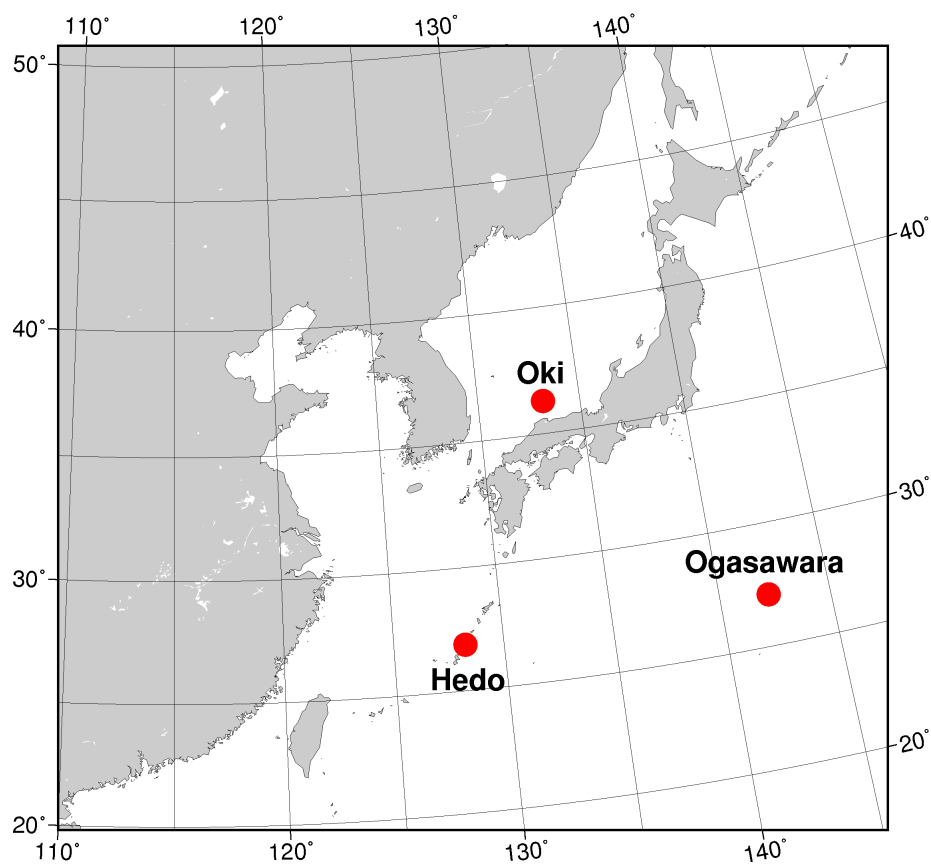


Fig. 1 Locations of EANET observation sites at Oki, Hedo and Ogasawara

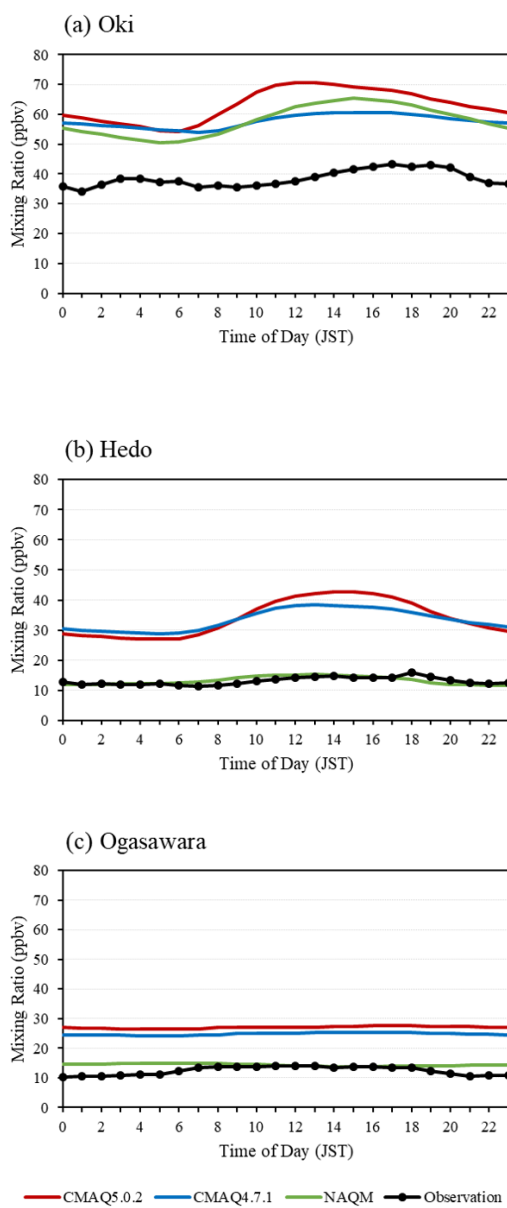


Fig. 2 Comparison of monthly-averaged diurnal variation in O_3 at (a) Oki, (b) Hedo, and (c) Ogasawara in July 2010 between observation and model simulation by CMAQ v.5.0.2 and 4.7.1, NAQM v.3.

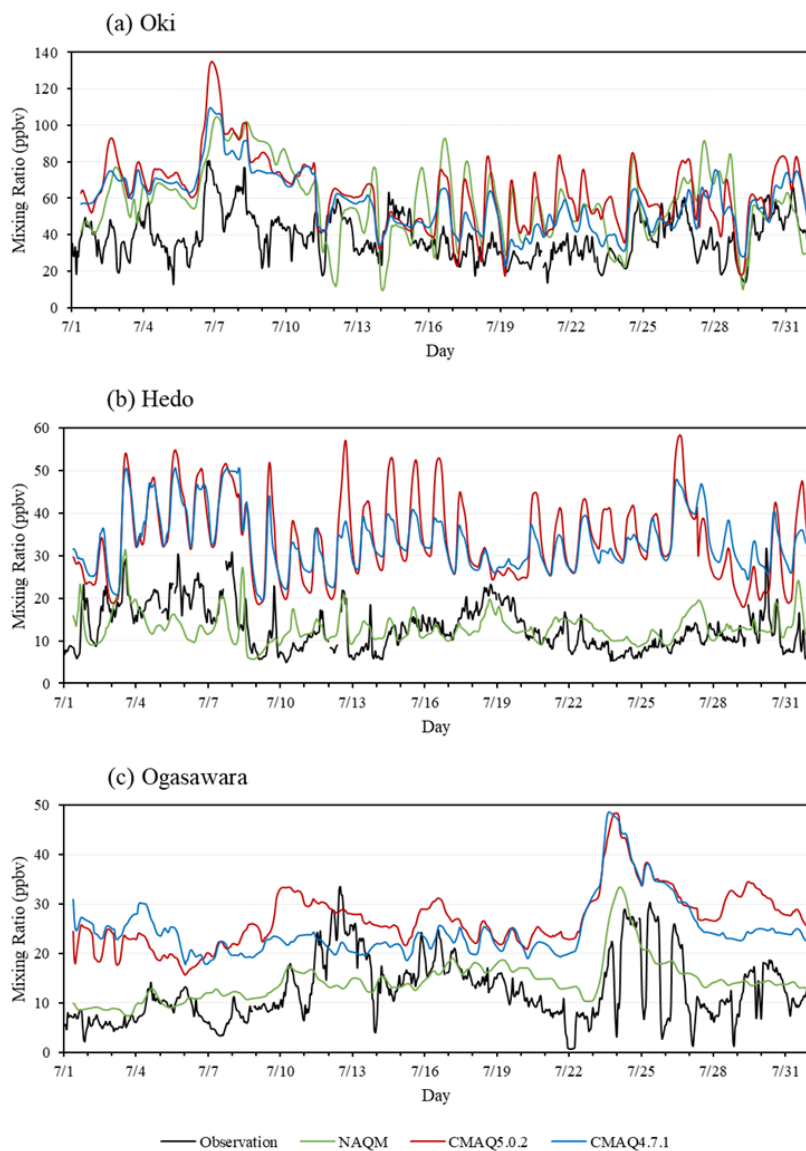


Fig. 3 Comparison of diurnal variation of surface O₃ mixing ratios at (a) Oki, (b) Hedo, and (c) Ogasawara in July, 2010 between observation and model simulation by CMAQ v.5.0.2 and v. 4.7.1 and NAQM v.3. Note that vertical scale is different for Oki and Hedo/Ogasawara.

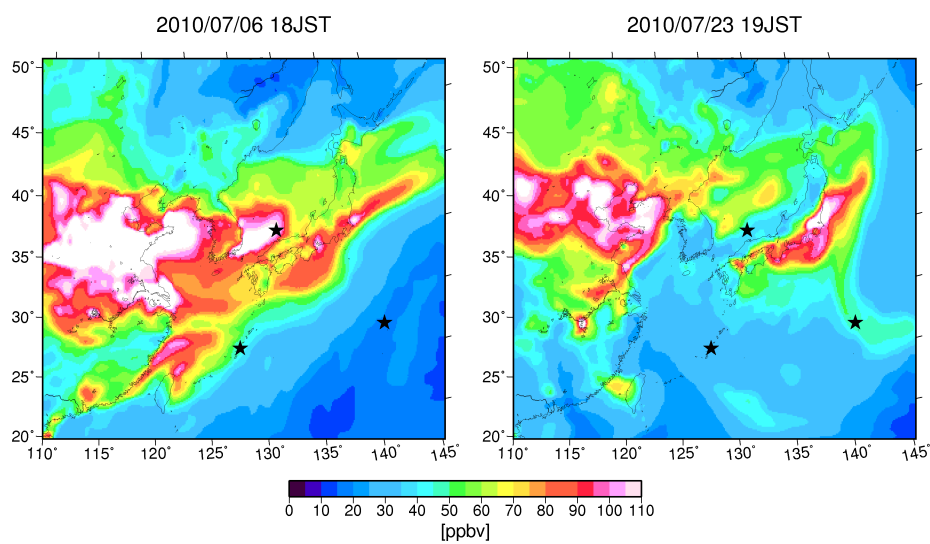


Fig. 4 Spatial distribution of surface O_3 over Northeast Asia at (a) 18 JST on July 6, and (b) 19 JST on July 23, 2010 simulated by CMAQ 4.7.1.

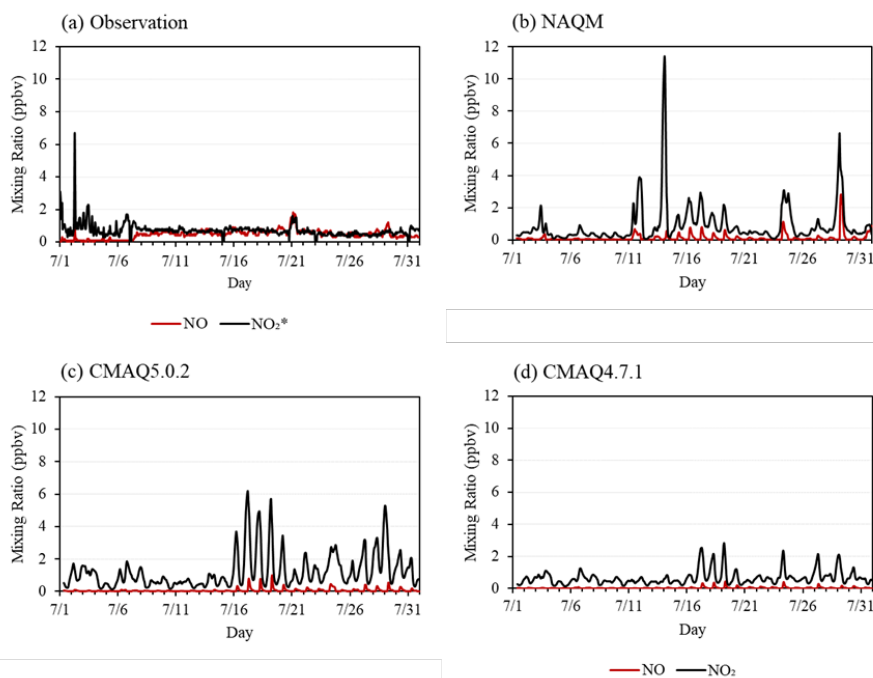


Fig. 5 Mixing Ratios of (a) NO_2^* and NO by observation, and NO_2 and NO by observation, and NO_2 and NO by model simulation by (b) NAQM, (c) CMAQ v.5.0.2, and (d) CMAQ v. 4.7.1, at Oki in July 2010.

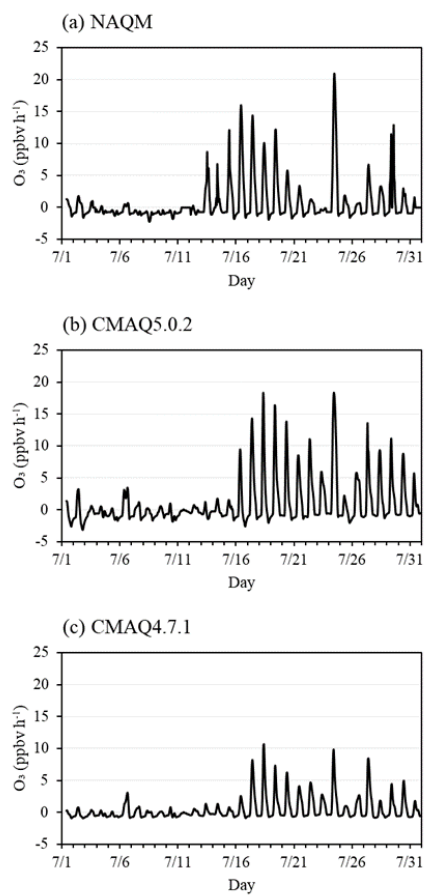


Fig. 6 Model-calculated net chemical production of O₃ at Oki in July 2010 by (a) NAQM, (b) CMAQ5.0.1 and (c) CMAQ 4.7.1.

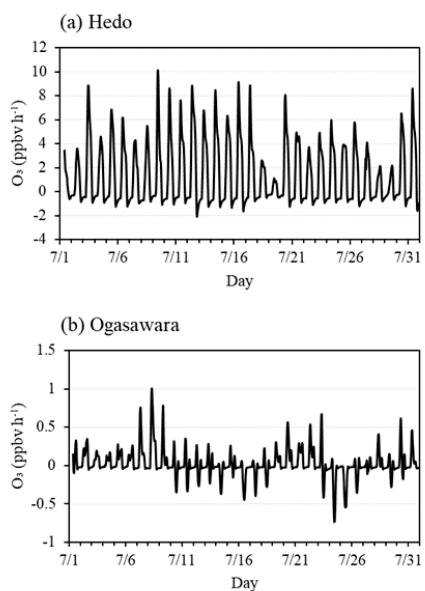


Fig. 7 Model-calculated net chemical production of O_3 in July 2010 by CMAQ 5.0.2 at (a) Hedo and (b) Ogasawara.

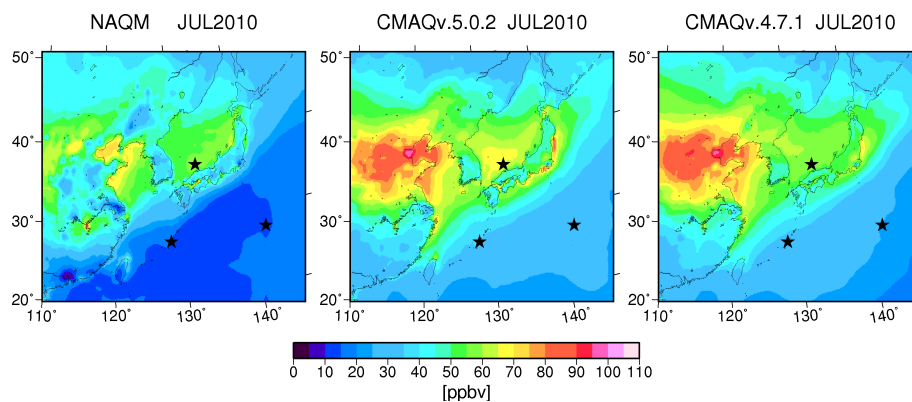


Fig. 8 Comparison of spatial distribution of surface O_3 mixing ratios in East Asia in July simulated by (a) NAQM, (b) CMAQ 5.0.2, and (c) 4.7.1.

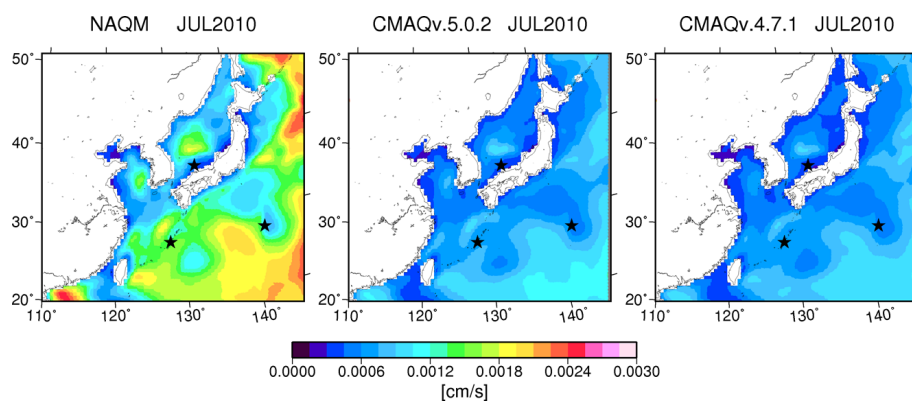


Fig. 9 Comparison of spatial distribution of dry deposition velocity of O_3 in East Asia simulated by (a) NAQM, (b) CMAQ 5.0.2, and (c) 4.7.1.